

AI based control theory for interaction of ocean system

C.-Y.J. Chen¹, Chia-Yen Hsieh², Aiden Smith³, Dariush Alako⁴,
Lallit Pandey⁵ and Tim Chen^{*6}

¹Department of Civil Engineering, Universidade de Brasília, Brasília, 70910-900 Distrito Federal, Brazil

²Special Education, National Kaohsiung Normal University, Kaohsiung

³Faculty of Engineering, Universidad del Norte, Barranquilla, AA 1569 Atlantico, Colombia

⁴Department of Natural Science, Bost University, Lashkargah Helmand, Afghanistan Afghanistan

⁵Applied Math Department, St. George's University, Grenada

⁶AI Lab, Faculty of Information Technology, Ton Duc Thang University, Ho Chi Minh City, Vietnam

(Received December 9, 2019, Revised March 20, 2020, Accepted March 27, 2020)

Abstract. This paper deals with the problem of the global stabilization for a class of tension leg platform (TLP) nonlinear control systems. Problem and objective: Based on the relaxed method, the chaotic system can be stabilized by regulating appropriately the parameters of dither. Scope and method: If the frequency of dither is high enough, the trajectory of the closed-loop dithered chaotic system and that of its corresponding model—the closed-loop fuzzy relaxed system can be made as close as desired. Results and conclusion: The behavior of the closed-loop dithered chaotic system can be rigorously predicted by establishing that of the closed-loop fuzzy relaxed system.

Keywords: intelligent control function; chaotic relaxed form; automated design

1. Introduction

Tension leg platform (TLP) is a "vertical mooring" floating structure commonly used in oil exploration and marine thermal energy conversion. This structure has also been used in aquatic environments with floating breakwaters (Harms 1979). The platform is permanently fixed by "tether" or "tendon" groups at each corner of the structure. One set of tethers is called "tensioned legs." A typical tensioned leg platform typically includes a buoyant body anchored to the ocean floor through pre-tensioned legs. The working platform on the semi-immersed floating body can be made of different materials. Simplified models with linear elasticity have been considered in previous studies (Lee and Wang 2001). In the case of estimating no tension, the movement or motion of the tether is reduced to an online rigid body motion proportional to the top of the platform when estimating the pretension force. The ultimate impact of resistance on TLP systems raises another important issue. In their research, TLP is affected by both surge motion caused by waves and resistance motion caused by flow, from which the overall resistance surge motion of TLP can be determined. Research results indicate that tether dragging can significantly reduce the TLP response (Lee and Wang 2003). However, in these studies, only the surge motion on the platform is considered

*Corresponding author, Dr., E-mail: timchen@tdtu.edu.vn

in the interaction between the wave and the platform structure.

After the pioneering work of Ott, Grebogi and Yorke (OGY) (Ott, Grebogi and Yorke 1990), controlling chaos has become a challenging topic in the field of nonlinear dynamics (Chen 2014a, b). Lately, fluffly rationale control (FLC) has been utilized in numerous fruitful useful control applications. In spite of the achievement, it has turned out to be obvious that numerous fundamental issues stay to be additionally tended to. In this paper, the Takagi-Sugeno (T-S) fluffly powerful model is made and this straightforward and general demonstrating technique endeavors to express each fluffly ramification by a direct framework display. This enables us to utilize straight criticism control strategies as on account of input adjustment. The idea of the parallel conveyed remuneration (PDC) conspire presented in Wang *et al.* (1996) is used to structure a fluffly controller to balance out the fluffly model. The thought is to structure a compensator for each standard of the fluffly model. Since each control rule is independently planned from the comparing principle of the T-S fluffly model, the direct control structure strategies can be utilized to plan the PDC fluffly controller. The subsequent by and large fluffly controller, which is commonly nonlinear, is a fluffly mixing of every individual direct controller. The fluffly controller for each standard offers the equivalent fluffly sets with the fluffly model in the start parts.

A few strategies for assessing solidness plans have been effectively connected, see Loria and Nesic (2003), Sontag (1989). Computational insight methodologies, for example, neural systems and fluffly frameworks have additionally been utilized to show dynamic marvels and applications in various regions. These apparatuses have turned out to be amazing and compelling. A few of the later works utilizing these methodologies can likewise be seen. Then again, calculations in swarm insight are likewise broadly used to build the reenactment model of a framework or to give ideal answers for issues in assembling, booking, and coordination in business, back, and designing. For moment, Chu and Tsai (2007) build up a lot of populace based learning rules for an Endless Drive Reaction (IIR) framework; Pardhan and Panda (2012) additionally use cat swarm optimization (CSO) to tackle numerous goal issues. Also, Wang *et al.* (1996) utilize CSO to enhance the data concealing outcomes. Intelligent Counterfeit Honey bee Settlement (IABC), which is proposed by Tsai *et al.* (2009), is effectively used to enhance the acknowledgment rate of the persistent confirmation framework (see Tsai *et al.* 2012) and to estimate the patterns of the outside conversion scale (see Chang *et al.* 2014a); and Evolved Bat Algorithm (EBA) has been employed to illustrate its usability in providing the optimal recommended stock portfolio (see Chang *et al.* 2014).

Although there have been many successful applications of intelligent computation, there are still some drawbacks to using them in any control scheme. To the best of our knowledge, the analysis of stability of TLPs with the NN-fuzzy model has not yet been discussed. For this reason, a fuzzy Lyapunov method as well as a NN-fuzzy model for dealing with the stability problem of TLPs (see Harms 1979, Liu and Zhang 2003, Wang *et al.* 1996) is given at the beginning. Recently, Chen *et al.* (2019) presented a relaxed model for the stability analysis for the TLP system. From this we study suitable mathematical modeling for the TLP system and discuss the interaction between a deformable floating structure and surface wave motion by virtue of a partial differential equation as well as fuzzy logic theory. However, the algorithm of the artificial evolved process still needs improvement in the practical control problem.

Egresits *et al.* (1998) maintained knowledge is firmly associated with picking up adjusting capacities, thus such abilities are considered as crucial highlights of smart assembling frameworks. Various methodologies have been depicted to apply diverse machine learning strategies for assembling issues, beginning with standard enlistment in representative example and areas acknowledgment procedures in numerical, sub emblematic spaces. Counterfeit neural system (ANN)

based learning is the prevailing machine learning strategy in assembling lately. It cannot exclusively be utilized in characterization, and estimation, yet can likewise be utilized for dependability investigation. For instance, the nonlinear Markov bounce standard hereditary administrative system model can be built utilizing the repetitive neural systems (see Zhu *et al.* 2013). Be that as it may, essentially these arrangements have constrained modern acknowledgment on account of the 'discovery' idea of ANNs. The incorporation of neural and fluffly methods is dealt with and previous arrangements are investigated by Egresits *et al.* (1998). Narendra *et al.* (1998) depicted a clever current controller for the quick and adaptable control utilizing ANN and Fluffy Rationale worldview. Two strategies for altering the learning parameters are exhibited: A heuristic way to deal with assess the learning rate as a polynomial of a vitality work is considered and learning parameters are examined; then again, Fluffy rationale, hereditary calculations and neural systems are three prevalent man-made reasoning methods which are utilized in numerous applications generally. Attributable to their particular properties and favorable circumstances, they are being explored and coordinated to shape new models or methodologies in the regions of framework control right now. A direct mapping technique is utilized to encode the genetic algorithm (GA) chromosome, which involves the middle and width of the enrollment capacities, and furthermore the loads of the controller. Dynamic hybrid and change probabilistic rates are likewise connected for quicker union of the genetic algorithm (GA) evolution. The estimating framework involves information gathering, general example display, uncommon example model, and choice incorporation. A feed forward neural system with mistake back engendering (EBP) learning calculation is utilized to take in the time arrangement information, or quantitative factors in the general pattern model. This paper utilized fuzzy logic which is capable of learning to learn the experts' knowledge considering the effect of promotion on the sales. In recent years, the research interest regarding generalized rheological models (GRMs) is also increasing (see Lewandowski *et al.* 2012). By using a constellation of artificial intelligence technologies, electronic Warfare (EW) Support Measures (ESM) systems are evolving rapidly toward unmanned status. The implementation and applications techniques, for which adaptive self-governing non-cooperative target recognition is useful or necessary, form the focus of this discussion. Military and civilian applications abound for fixed site, ship borne, and airborne systems. These systems could control and manage other interactive systems normally needing manual inputs. Simoes *et al.* portrayed the control strategy development, experimental performance, and design e evaluation of a fuzzy-logic-based variable-speed wind generation system that uses a cage-type induction generator and double-sided pulse width-modulated converters (see Simoes *et al.* 1997). The system can feed a utility grid maintaining unity power factor at all conditions or can supply a self-governing load. The fuzzy-logic-based control of the system helps to optimize efficiency and improve performance. In metal processing industries, for this they applied on one hand an artificial neural network, which learns to categorize the data adequately by using given exemplary process states. Besides, they presented investigations of fuzzy clustering techniques to acquire information about the process. Furthermore, topology optimization by evolutionary algorithms is considered to acquire optimal structures of the multilayer perception used. On to the next hierarchical level, the quality features extracted are then passed, where they are processed within the framework of an integrated manufacturing and quality control system. A fuzzy-based neural network paradigm with an on-line learning algorithm is developed to execute expert advising for the ground-based maintenance crew. Hierarchical fault diagnosis architecture is advocated to perform on-board needs and the time-critical in different levels of structural integrity over a global operating envelope. In modern process automation, intelligent control has become a question of primary importance as it provides the prerequisites for the task of fault detection (see Tyan *et al.* 1996). The ability to detect the faults is important to improve

reliability and security of a complex control system. During recent years, parameter estimation methods, state observation schemes, statistical likelihood ratio tests, rule-based expert system reasoning, pattern recognition techniques, and artificial neural network approaches are the most common methodologies developed actively. Tyan *et al.* (1996) described a completed feasibility study demonstrating the merit of employing pattern recognition and an artificial neural network for error diagnosis through back propagation learning algorithm and making the use of fuzzy approximate reasoning for fault control via parameter changes in a dynamic system.

Some references of damage assessment and uncertainty analysis were published to mitigate the threaten of casualty, in which the fuzzy theory has received considerable attention recently in structural engineering. Various approaches have been developed for detecting damage based on various methods (see Egresits *et al.* 1998).

For intricate dynamical systems, in designing controllers there are needs that are not sufficiently addressed by conventional control theory (see Tyan *et al.* 1996). These relate mainly to the problem of environmental uncertainty and often call for human-like decision making needing the use of heuristic reasoning and learning experience. Learning is needed complexity of a problem or the uncertainty thereof prevents a priori specification of a satisfactory solution. Such solutions are then only possible through gathering information about the problem and using this information to dynamically generate an acceptable solution. Such systems can be referred to as intelligent control systems. From integrating mechanical, software and electrical intelligence in minimum space, mechatronic components have become intelligent, certainly an important step. With a bright future, taking this and recent successes using artificial neural networks, fuzzy logic and genetic algorithms, so called soft computing, the field of IC is exciting. This article attempts to expect this future and discusses directions of research to approach the realization of more intelligent systems.

2. System description

2.1 Notations of variables

u : horizontal velocity component

w : vertical velocity component

ϕ : velocity potential

η : disturbance at the water level

h : water depth

F: any fixed or moving surface

z : location

t : time

λ : wavelength

A_i : wave amplitude

*: new non-dimensional variable

ρ : fluid density

p : wave pressure

g : gravitational acceleration

c : a parameter

$C(t)$: a function of time

L : wave length

T : wave period

k : wave number

σ : wave frequency

i : complex variable

r : coefficient of wave reflection

Total velocity potential ϕ I consists of incident waves ϕ i, scattered waves ϕ IS, motion radiation waves ϕ IW, and vibration radiation waves ϕ IV. Total velocity potentials ϕ II and ϕ III consist of both scattered, ϕ IIS and ϕ IIIS, and radiated waves, ϕ IIW, ϕ IIIW, ϕ IIV, and ϕ IIIV, where the subscript ‘‘S’’ denotes the scattering problem, ‘‘W’’ the wave-maker (i.e., primitive radiation) problem induced by surge motion, and ‘‘V’’ the vibration radiation problem induced by the platform deformation. The boundary value problems correspond to the scattering and radiation problems. The displacement from surge motion with unknown amplitude S is given by $\bar{X} = Se^{-i\sigma t}$, and the deformation of the platform on z -axis is defined as ζ , which is function of x and t .

2.2 Systematic modeling

Consider a wave-induced flow field system in which a Cartesian coordinate system is employed. As shown in the sketch of a 2D numerical wave flume, a plane $z=0$ coincides with the undisturbed still water level and the z -axis is directed vertically upward. The vertical elevation of any point on the free surface can be defined by the function $z = \eta(x, y, t)$, in which the surface tension is negligible.

Eq. (1) is used to described the Dynamic boundary conditions

$$\left\{ \begin{array}{l} \eta_{IS} = -\frac{1}{g} \frac{\partial \Phi_{IS}}{\partial t} \\ \eta_{IW} = -\frac{1}{g} \frac{\partial \Phi_{IW}}{\partial t} \end{array} \right. \text{ on } z=0, \left\{ \begin{array}{l} \frac{\partial \Phi_{IS}}{\partial t} = \frac{\partial \Phi_{IIS}}{\partial t} \\ \frac{\partial \Phi_{IW}}{\partial t} = \frac{\partial \Phi_{IIW}}{\partial t} \end{array} \right. \begin{array}{l} -h \leq z \leq -d \\ -h \leq z \leq -d \end{array} \text{ on } x=-b; \quad (1)$$

And Eq. (2) is used to describe Radiation condition

$$\lim_{x \rightarrow \infty} \left[\frac{\partial \Phi_{IS}}{\partial x} - \frac{1}{c} \frac{\partial \Phi_{IS}}{\partial t} \right] = 0 \quad (2)$$

In order to solve the chaotic scenario, the algorithm for constructing the dither signal is given as follows (Steinberg and Kadushin 1973): The time interval is divided into an arbitrary number V of equal subintervals. The beginning of the first interval, the end of the first interval, the end of the second interval is applied at the m th subinterval.

Hence the repetition frequency, shape and amplitude of dither can be determined by regulating the parameters in order to illustrated the algorithm.

Remark 1: According to this algorithm, we have that if the dither is chosen to be a periodic signal then the parameters $\alpha_m(t)$ and $\beta_m(t)$ are independent of time.

The corresponding relaxed model of the dithered chaotic system is defined as (Steinberg and

Kadushin 1973)

$$\dot{x}_R(t) = \sum_{m=1}^n \alpha_m(t) f(x_R, u_R, \beta_m) \tag{3}$$

which is non-negative and satisfies $0 \leq \alpha_m(t) \leq 1, \sum_{m=1}^n \alpha_m(t) = 1$

The momentum equation obtained from the motion of the floating structure is extensively derived from Newton's second law. Assume that the momentum equation of a TLP system can be characterized by the following differential equation

$$M\ddot{\bar{X}}(t) = -M\bar{r}\phi(t) \tag{4}$$

where $\bar{X}(t) = [\bar{x}_1(t), \bar{x}_2(t) \dots \bar{x}_n(t)] \in R^n$ is an n-vector; $\ddot{\bar{X}}(t), \dot{\bar{X}}(t), \bar{X}(t)$ are the acceleration, velocity, and displacement vectors, respectively. This is only a static model and M is the mass of the system; $M\bar{r}\phi(t)$ is a wave-induced external force which can be expressed as follows

$$M\bar{r}\phi(t) = F_{wx} - F_{Tx} \tag{5}$$

where F_{wx} is the horizontal wave force acting on the both sides of the structure; and F_{Tx} is the horizontal component of the static (or the pre-tensioned) tension applied by the tension legs. The static tension is given by $F_{Tx} = f\xi$.

$$\text{IF } x_{R1}(t) \text{ is } M_{Ri1}(\alpha_m, \beta_m) \text{ and ... and } x_{Rk}(t) \text{ is } M_{Rik}(\alpha_m, \beta_m) \text{ THEN} \tag{6}$$

Thus, the overall fuzzy controller and fuzzy observer can be written as

$$u_R(t) = - \frac{\sum_{i=1}^r w_i(x_R(t), \alpha_m, \beta_m) K_i \hat{x}_R(t)}{\sum_{i=1}^r w_i(x_R(t), \alpha_m, \beta_m)} \tag{7}$$

$$\dot{\hat{x}}_R(t) = \frac{\sum_{i=1}^r w_i(x_R(t), \alpha_m, \beta_m) \{A_i(\alpha_m, \beta_m) \hat{x}_R(t) + B_i(\alpha_m, \beta_m) u_R(t) + L_i(y_R(t) - \hat{y}_R(t))\}}{\sum_{i=1}^r w_i(x_R(t), \alpha_m, \beta_m)} \tag{8}$$

where

$$\hat{y}_R(t) = \frac{\sum_{i=1}^r w_i(x_R(t), \alpha_m, \beta_m) D_i(\alpha_m, \beta_m) \hat{x}_R(t)}{\sum_{i=1}^r w_i(x_R(t), \alpha_m, \beta_m)} \tag{9}$$

For controller design as proposed by Sontag (1989), Park et al. (2001), and Sun et al. (2003), the standard first-order state equation is assuming the equation of motion for a shear-type-building modeled by an n-degrees-of-freedom system controlled by actuators and subjected to an external force $\phi(t)$

$$\dot{X}(t) = AX(t) + E\phi(t) \tag{10}$$

where $X(t) = \begin{bmatrix} \bar{x}(t) \\ \dot{\bar{x}}(t) \end{bmatrix}$, $A = \begin{bmatrix} 0 & I \\ -M^{-1}K & -M^{-1}C \end{bmatrix}$, $E = \begin{bmatrix} 0 \\ -\bar{r} \end{bmatrix}$, in which $\bar{X}(t) = [\bar{x}_1(t), \bar{x}_2(t) \dots \bar{x}_n(t)] \in R^n$ is an n-vector; $\ddot{\bar{X}}(t)$, $\dot{\bar{X}}(t)$, $\bar{X}(t)$ are the acceleration, velocity, and displacement vectors, respectively; matrices M, C, and K are mass, damping, and stiffness matrices, respectively; \bar{r} is an n-vector denoting the influence of the external force; $\phi(t)$ is the excitation with a upper bound; U(t) corresponds to the actuator forces (generated via active a tendon system or an active mass damper, for example). This is only a static model is a state vector; A is a system matrix. Because of the simplification and systematic design, the fuzzy rules of the controller are presented.

A neural-network-based model can be described as follows

$$\dot{X}(t) = \Psi^S (W^S \Psi^{S-1} (W^{S-1} \Psi^{S-2} (\dots \Psi^2 (W^2 \Psi^1 (W^1 \Lambda(t))) \dots))) \tag{11}$$

It is assumed that $w_i(t) \geq 0$, \tag{12}

Theorem 1: The augmented system is asymptotically stable in the large if there exists a common positive definite matrix \tilde{P} , the controller gains K_i and observer gains L_i can be found to satisfy the following matrix inequalities

$$\tilde{A}_{ii}^T(\alpha_m, \beta_m) \tilde{P} + \tilde{P} \tilde{A}_{ii}(\alpha_m, \beta_m) < 0, \quad i = 1, 2, \dots, r \tag{13}$$

Proof- A

X=-b (K.B.C)

$$\frac{k_\alpha \langle z_\alpha z_\alpha \rangle}{\cos(k_\alpha h)} A_{1s\alpha} - i \left[\frac{1}{b} \langle z_{21} z_\alpha \rangle^d A_{2s1} + \sum_{n=2}^{\infty} (-1)^{n-1} K_{2n} \langle z_{2n} z_\alpha \rangle^d (-A_{2Sn} + B_{2Sn} e^{-K_{2n} b}) \right] = \delta_{\alpha 1} e^{K_{1b}} \frac{K_1 \langle z_1 z_1 \rangle}{\cos(k_1 h)} A_1 \tag{A-1}$$

X=+b (KBC)

$$i \left[\frac{1}{b} \langle z_{21} z_{2\alpha} \rangle^d A_{2S1} + \sum_{n=2}^{\infty} (-1)^{n-1} K_{2n} \langle z_{2n} z_{2\alpha} \rangle^d (A_{2Sn} e^{-K_{2n}b} + B_{2Sn}) \right] + \frac{K_{\alpha} \langle z_{\alpha} z_{\alpha} \rangle}{\cos(K_{\alpha}h)} A_{3S\alpha} = 0 \tag{A-2}$$

X=-b (DBC)

$$-i \sum_{n=1}^{\infty} \frac{\langle z_n z_{2\alpha} \rangle^d}{\cos(K_n h)} A_{1Sn} - \langle z_{2\alpha} z_{2\alpha} \rangle \{ [(1 - \delta_{\alpha 1})(-1)^{\alpha-1} - \delta_{\alpha 1}] A_{2Sn} + [(1 - \delta_{\alpha 1})(-1)^{\alpha-1} + \delta_{\alpha 1}] e^{-2K_{2\alpha}b} B_{2Sn} \} = 0 \tag{A-3}$$

X=+b (DBC)

$$\{ [(1 - \delta_{\alpha 1})(-1)^{\alpha-1} + \delta_{\alpha 1}] (A_{2Sn} e^{-2K_{2\alpha}b} + B_{2Sn}) \} + i \sum_{n=1}^{\infty} \frac{\langle z_n z_{2\alpha} \rangle^d}{\cos(K_n h)} B_{3Sn} = 0 \tag{A-4}$$

Proof- B

X=-b (KBC)

$$\frac{K_{\alpha} \langle z_{\alpha} z_{\alpha} \rangle}{\cos(K_{\alpha}h)} A_{1W\alpha} - i \left[\frac{1}{b} \langle z_{21} z_{2\alpha} \rangle^d A_{2W1} + \sum_{n=2}^{\infty} (-1)^{n-1} K_{2n} \langle z_{2n} z_{2\alpha} \rangle^d (-A_{2Wn} + B_{2Wn} e^{-K_{2n}b}) \right] - \frac{i\sigma^2}{g} \langle z_{\alpha}^0 \rangle^d S = 0 \tag{B-1}$$

X=-b (DBC)

$$-i \sum_{n=1}^{\infty} \frac{\langle z_n z_{2\alpha} \rangle^d}{\cos(K_n h)} A_{1Wn} - \langle z_{2\alpha} z_{2\alpha} \rangle \{ [(1 - \delta_{\alpha 1})(-1)^{\alpha-1} - \delta_{\alpha 1}] A_{2Wn} + [(1 - \delta_{\alpha 1})(-1)^{\alpha-1} + \delta_{\alpha 1}] e^{-2K_{2\alpha}b} B_{2Wn} \} = 0 \tag{B-2}$$

X=+b (KBC)

$$\frac{K_{\alpha} \langle z_{\alpha} z_{\alpha} \rangle}{\cos(K_{\alpha}h)} A_{1W\alpha} - i \left[\frac{1}{b} \langle z_{21} z_{2\alpha} \rangle^d A_{2W1} + \sum_{n=2}^{\infty} (-1)^{n-1} K_{2n} \langle z_{2n} z_{2\alpha} \rangle^d (-A_{2Wn} + B_{2Wn} e^{-K_{2n}b}) \right] - \frac{i\sigma^2}{g} \langle z_{\alpha}^0 \rangle^d S = 0 \tag{B-3}$$

X=+b (DBC)

$$\langle z_{2\alpha} z_{2\alpha} \rangle \{ [(1 - \delta_{\alpha 1})(-1)^{\alpha-1} - \delta_{\alpha 1}] A_{2Wn} + [(1 - \delta_{\alpha 1})(-1)^{\alpha-1} + \delta_{\alpha 1}] e^{-2K_{2\alpha}b} B_{2Wn} \} + i \sum_{n=1}^{\infty} \frac{\langle z_n z_{2\alpha} \rangle^d}{\cos(K_n h)} B_{3Wn} = 0 \tag{B-4}$$

Momentum equation

$$\bar{B}_n \sum_{i=1}^r h_i(t) K_i X(t) + \rho \int_{-d}^0 \left[\frac{\partial \phi_I}{\partial t} \Big|_{x=-b} - \frac{\partial \phi_{III}}{\partial t} \Big|_{x=b} \right] dz - f\xi = -M(-i\sigma)^2 S e^{-i\sigma t} \tag{B-5}$$

Substituting the velocity potentials into the (B-5) yields

$$\int_{-d}^0 \left[\sum_{n=1}^{\infty} \frac{\cos K_n(h+z)}{\cos K_n h} (A_{1Wn} - A_{3Wn}) \right] dz + \frac{i(M\sigma^2 - f)S}{\rho g} + \int_{-d}^0 \left[\sum_{n=1}^{\infty} \frac{\cos K_n(h+z)}{\cos K_n h} (A_{1Vn} - A_{3Vn}) \right] dz$$

$$= \int_{-d}^0 \left[\frac{\cos K_1(h+z)}{\cos K_1 h} e^{k_1 b} A_i + \sum_{n=1}^{\infty} \frac{\cos K_n(h+z)}{\cos K_n h} (A_{1Sn} - A_{3Sn}) \right] dz + \bar{B}_n \sum_{i=1}^r h_i(t) K_i X(t) \tag{B-6}$$

where A_{1Vn}, B_{3Vn} are unknown parameters.

Proof- C

X=-b(K.B.C)

$$\frac{k_{\alpha} \langle z_{\alpha} z_{\alpha} \rangle}{\cos(k_{\alpha} h)} A_{1\alpha} - i \left[\frac{1}{b} \langle z_{21} z_{\alpha} \rangle^d A_{2V1} + \sum_{n=2}^{\infty} (-1)^{n-1} K_{2n} \langle z_{2n} z_{\alpha} \rangle^d (-A_{2Vn} + B_{2Vn} e^{-K_{2n} b}) \right]$$

$$- \frac{\sigma}{g} D_{2V1} \lambda_l \langle Z_{\lambda l} Z_{\alpha} \rangle = 0 \tag{C-1}$$

X=+b (KBC)

$$i \left[\frac{1}{b} \langle z_{21} z_{\alpha} \rangle^d A_{2V1} + \sum_{n=2}^{\infty} (-1)^{n-1} K_{2n} \langle z_{2n} z_{\alpha} \rangle^d (A_{2Vn} e^{-K_{2n} b} + B_{2Vn}) \right] + \frac{K_{\alpha} \langle z_{\alpha} z_{\alpha} \rangle}{\cos(K_{\alpha} h)} A_{3V\alpha}$$

$$- \frac{\sigma}{g} (-1)^l D_{2V1} \lambda_l \langle Z_{\lambda l} Z_{\alpha} \rangle = 0 \tag{C-2}$$

X=-b (DBC)

$$-i \sum_{n=1}^{\infty} \frac{\langle z_n z_{2\alpha} \rangle^d}{\cos(K_n h)} A_{1Vn} - \langle z_{2\alpha} z_{2\alpha} \rangle \left\{ [(1 - \delta_{\alpha 1})(-1)^{\alpha-1} - \delta_{\alpha 1}] A_{2Vn} \right.$$

$$\left. + [(1 - \delta_{\alpha 1})(-1)^{\alpha-1} + \delta_{\alpha 1}] e^{-2K_{2n} b} B_{2Vn} \right\} = 0 \tag{C-3}$$

X=+b (DBC)

$$\left\{ [(1 - \delta_{\alpha 1})(-1)^{\alpha-1} + \delta_{\alpha 1}] (A_{2Vn} e^{-2K_{2n} b} + B_{2Vn}) \right\} + i \sum_{n=1}^{\infty} \frac{\langle z_n z_{2\alpha} \rangle^d}{\cos(K_n h)} B_{3Vn} = 0 \tag{C-4}$$

Deformable TLP equation

$$M \frac{\partial^2 \zeta(x,t)}{\partial^2 t} + EI \frac{\partial^4 \zeta(x,t)}{\partial^4 x} = p(x,t) \tag{C-5}$$

in which p wave pressure is composed of Ps, Pv, and Pw. A TLP can be regarded as deformable due to harmonic motion as expressed by

$$P_S(x,t) = -i\sigma\phi_{lls}(x,-d)e^{-i\sigma t} \tag{C-6}$$

$$P_V(x,t) = -i\sigma \sum_{l=1}^{\infty} A_l \phi_{IV}(x,-d) e^{-i\sigma t} \tag{C-7}$$

$$P_W(x,t) = -i\sigma \phi_{IW}(x,-d) e^{-i\sigma t} \tag{C-8}$$

$$\zeta(x,t) = -\sum_{l=1}^{\infty} A_l f_l(x) e^{-i\sigma t}, \quad f_l(x) = \sin \lambda_l(x+b) \tag{C-9}$$

Substituting (C-6)-(C-9) into (C-5) yields

$$\sum_{l=1}^{\infty} A_l [K_{l\beta} - \sigma^2(M_{l\beta} - M_{al\beta}) - i\sigma C_{l\beta}] = P_{S\beta} + P_{W\beta} \tag{C-10}$$

in which the coefficients in (C-10) include

$$K_{l\beta} = \int_{-b}^{+b} (EIf_l'''(x)) f_{\beta}(x) dx \tag{C-11}$$

$$M_{l\beta} = \int_{-b}^{+b} M f_{\beta}(x) dx \tag{C-12}$$

$$M_{al\beta} = \text{Re} \left[\frac{1}{\sigma^2} \int_{-b}^{+b} P_{2lV}(x) f_{\beta}(x) dx \right] \tag{C-13}$$

$$C_{l\beta} = \text{Im} \left[\frac{1}{\sigma} \int_{-b}^{+b} P_{2lV}(x) f_{\beta}(x) dx \right] \tag{C-14}$$

$$P_{S\beta} = \int_{-b}^{+b} P_S(x) f_{\beta}(x) dx \tag{C-15}$$

$$P_{W\beta} = \int_{-b}^{+b} P_W(x) f_{\beta}(x) dx \tag{C-16}$$

$$P_{S\beta} = \rho g \left\{ A_{2s1} \langle Z_0 Z_{\lambda\beta} \rangle + B_{2s1} \langle Z_x Z_{\lambda\beta} \rangle + \sum_{n=2}^{\infty} (-1)^{n-1} \left[A_{2sn} \langle Z_{Kb} Z_{\lambda\beta} \rangle + B_{2sn} \langle Z_{-Kb} Z_{\lambda\beta} \rangle \right] \cos K_{2n}(h-d) \right\} \tag{C-17}$$

$$P_{W\beta} = \rho g \left\{ A_{2w1} \langle Z_0 Z_{\lambda\beta} \rangle + B_{2w1} \langle Z_x Z_{\lambda\beta} \rangle + \sum_{n=2}^{\infty} (-1)^{n-1} \left[A_{2wn} \langle Z_{Kb} Z_{\lambda\beta} \rangle + B_{2wn} \langle Z_{-Kb} Z_{\lambda\beta} \rangle \right] \cos K_{2n}(h-d) \right\} \tag{C-18}$$

$$M_{al\beta} = \frac{1}{\sigma^2} \text{Re} \left[\rho g \left\{ A_{2v1} \langle Z_0 Z_{\lambda\beta} \rangle + B_{2v1} \langle Z_x Z_{\lambda\beta} \rangle + \sum_{n=2}^{\infty} (-1)^{n-1} \left[A_{2vn} \langle Z_{Kb} Z_{\lambda\beta} \rangle + B_{2vn} \langle Z_{-Kb} Z_{\lambda\beta} \rangle \right] \cos K_{2n}(h-d) \right\} - i\sigma g D_{2vl} \cosh \lambda_{\beta}(h-d) \langle Z_{\lambda l} Z_{\lambda\beta} \rangle \right] \tag{C-19}$$

$$C_{l\beta} = \frac{1}{\sigma} \text{Im} \left[\rho g \left\{ A_{2v1} \langle Z_0 Z_{\lambda\beta} \rangle + B_{2v1} \langle Z_x Z_{\lambda\beta} \rangle + \sum_{n=2}^{\infty} (-1)^{n-1} \left[A_{2wn} \langle Z_{kb} Z_{\lambda\beta} \rangle + B_{2wn} \langle Z_{-kb} Z_{\lambda\beta} \rangle \right] \cos K_{2n} (h-d) \right\} - i \sigma g D_{2v1} \cosh \lambda_{\beta} (h-d) \langle Z_{\lambda l} Z_{\lambda\beta} \rangle \right] \quad (\text{C-20})$$

Proof- D

Using the Lyapunov function candidate for the system

$$V = X^T(t) P X(t) \quad (\text{D-1})$$

The time derivative of V is

$$\dot{V} = \dot{X}^T(t) P X(t) + X^T(t) P \dot{X}(t)$$

$$= \left\{ \sum_{i=1}^r \sum_{l=1}^r h_i(t) h_l(t) [A_i X(t) + E_i \phi(t)]^T P X(t) + X^T(t) P \left\{ \sum_{i=1}^r \sum_{l=1}^r h_i(t) h_l(t) [A_i X(t) + E_i \phi(t)] \right\} \right. \quad (\text{D-2})$$

$$= \sum_{i=1}^r \sum_{l=1}^r h_i(t) h_l(t) X^T(t) [A_i^T P + P A_i] X(t) + \phi^T(t) E_i^T P X(t) + X^T(t) P E_i \phi(t) - [\eta^2 \phi^T(t) \phi(t) + \frac{1}{\eta^2} X^T(t) P E_i E_i^T P X(t)]^* + \left[\eta^2 \phi^T(t) \phi(t) + \frac{1}{\eta^2} X^T(t) P E_i E_i^T P X(t) \right] \quad (\text{D-3})$$

$$\leq \sum_{i=1}^r \sum_{l=1}^r h_i(t) h_l(t) X^T(t) [A_i^T P + P A_i + \frac{1}{\eta^2} P E_i E_i^T P] X(t) + \eta^2 \|\phi_{up}(t)\|^2 \quad (\text{D-4})$$

Based on the Theorem, the proof is thereby completed.

3. The experiment design and the simulation result

According to theorem 1, it provides a useful criterion that ensures the system response is stable in the large. Base on theorem 1, selecting the proper common positive definite matrix P and the control force K becomes the key problem to be dealt with. In this paper, we use EBA to discover the proper solutions. In this case, the obtained solutions can be classified into two categories: feasible and infeasible. However, the limitation is not applied for the matrix K because the total effect contributed to the whole system by the control force is relatively small. The solutions found by the

The * could be represented as $-\left(\frac{1}{\eta} (P E_i)^T X(t) - \eta \phi(t)\right)^T \left(\frac{1}{\eta} (P E_i)^T X(t) - \eta \phi(t)\right) < 0$.

EBA are determined as feasible if the eigen values are all negative, because the negative eigen values result in the control system staying stable in the large. Table 1 shows 10 samples from overall feasible solutions found by EBA with the corresponding eigen values.

By combining the whole set of fuzzy rules, the approximation of the TLP system is completed. Thus, the fuzzy model approximated TLP nonlinear system can be described. The evaluation criterion for determining the fitness of a bat is based on a user defined fitness function. A fitness function is employed in the paper to find the common symmetric positive definite matrix and the control force of the controller.

Table 1 Samples of the obtained feasible solutions by EBA with system eigen values

	Matrices P and K	Eigen Values	
		with A_1, B_1	with A_2, B_2
Set 1	$P = \begin{bmatrix} 3.2641 & 0.6081 \\ 0.6081 & 0.9971 \end{bmatrix}, K^T = \begin{bmatrix} -1.4172 \\ -0.1151 \end{bmatrix}$	$\begin{bmatrix} -8.1912 \\ -2.1826 \end{bmatrix}$	$\begin{bmatrix} -9.2384 \\ -1.7674 \end{bmatrix}$
Set 2	$P = \begin{bmatrix} 3.8752 & 0.3773 \\ 0.3773 & 1.0645 \end{bmatrix}, K^T = \begin{bmatrix} -1.6726 \\ -0.2747 \end{bmatrix}$	$\begin{bmatrix} -12.9525 \\ -1.6175 \end{bmatrix}$	$\begin{bmatrix} -7.6539 \\ -1.9006 \end{bmatrix}$
Set 3	$P = \begin{bmatrix} 3.9862 & 0.6328 \\ 0.6328 & 0.3880 \end{bmatrix}, K^T = \begin{bmatrix} -1.6705 \\ -0.2633 \end{bmatrix}$	$\begin{bmatrix} -9.1133 \\ -1.9422 \end{bmatrix}$	$\begin{bmatrix} -6.5002 \\ -1.0776 \end{bmatrix}$
Set 4	$P = \begin{bmatrix} 3.4095 & 0.3250 \\ 0.3250 & 0.5086 \end{bmatrix}, K^T = \begin{bmatrix} -1.4341 \\ -0.0744 \end{bmatrix}$	$\begin{bmatrix} -2.9977 \\ -2.0886 \end{bmatrix}$	$\begin{bmatrix} -3.3554 \\ -2.3777 \end{bmatrix}$
Set 5	$P = \begin{bmatrix} 4.6075 & 0.6311 \\ 0.6311 & 0.7700 \end{bmatrix}, K^T = \begin{bmatrix} -1.4033 \\ -0.3754 \end{bmatrix}$	$\begin{bmatrix} -9.0082 \\ -3.9219 \end{bmatrix}$	$\begin{bmatrix} -6.8969 \\ -2.9625 \end{bmatrix}$
Set 6	$P = \begin{bmatrix} 4.4938 & 0.6361 \\ 0.6361 & 1.4047 \end{bmatrix}, K^T = \begin{bmatrix} -1.4631 \\ -0.7790 \end{bmatrix}$	$\begin{bmatrix} -29.3484 \\ -3.0169 \end{bmatrix}$	$\begin{bmatrix} -11.5857 \\ -2.2598 \end{bmatrix}$
Set 7	$P = \begin{bmatrix} 3.0719 & 0.0864 \\ 0.0864 & 0.9208 \end{bmatrix}, K^T = \begin{bmatrix} -1.4645 \\ -1.9464 \end{bmatrix}$	$\begin{bmatrix} -39.6258 \\ -0.5657 \end{bmatrix}$	$\begin{bmatrix} -6.3168 \\ -0.2100 \end{bmatrix}$
Set 8	$P = \begin{bmatrix} 2.7318 & 0.2748 \\ 0.2748 & 0.3832 \end{bmatrix}, K^T = \begin{bmatrix} -1.3799 \\ -1.4559 \end{bmatrix}$	$\begin{bmatrix} -13.1626 \\ -1.1711 \end{bmatrix}$	$\begin{bmatrix} -2.8163 \\ -1.8329 \end{bmatrix}$
Set 9	$P = \begin{bmatrix} 2.1372 & 0.4420 \\ 0.4420 & 0.3884 \end{bmatrix}, K^T = \begin{bmatrix} -1.7609 \\ -0.9665 \end{bmatrix}$	$\begin{bmatrix} -13.6180 \\ -1.4539 \end{bmatrix}$	$\begin{bmatrix} -4.9761 \\ -1.0774 \end{bmatrix}$
Set 10	$P = \begin{bmatrix} 1.9452 & 0.1138 \\ 0.1138 & 0.4373 \end{bmatrix}, K^T = \begin{bmatrix} -1.3655 \\ 0.0301 \end{bmatrix}$	$\begin{bmatrix} -1.2705 \\ -0.8623 \end{bmatrix}$	$\begin{bmatrix} -2.6596 \\ -0.8972 \end{bmatrix}$

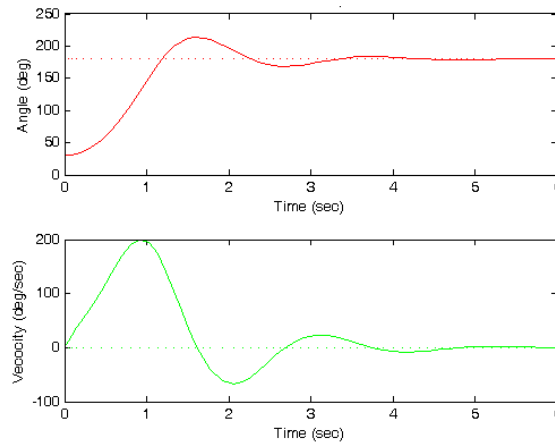


Fig. 1 The response of the system without control

A large population size provides a larger chance for the algorithm to find the near best solutions. However, a larger population size requires more memory resource and computation power. Hence, we set the population size to be 16 in the experiment. Fig. 1 shows the changes of the angle and the velocity of the without any control force. The simulation time is 6 seconds.

4. Conclusions

A fuzzy controller and a fuzzy observer are proposed via the parallel distributed compensation technique to stabilize the chaotic system. If the fuzzy controller and the fuzzy observer cannot asymptotically stabilize the chaotic system, a dither is injected into the chaotic system, just ahead of the nonlinearity. Then, the fuzzy controller, the fuzzy observer and the dither signal are simultaneously introduced to transfer the chaotic motions to the origin. Simulation results show that the fuzzy controller and the fuzzy observer can convert the chaotic motion into the origin by appropriately regulating the amplitude of dither when the dither's frequency is high enough. A simulation of the nonlinear system is given at the last. The experimental result indicates that EBA with our proposed fitness function presents a 93.77% success rate in average for finding the feasible solutions. Moreover, the dependence of wave reflection, transmission, and structural surge motion on incident wave conditions and structural characteristics has been demonstrated. The results show that the response of the floating structure is affected by the quality of the structure, which results in different contours of the wave motion.

References

- Bal, S. (2016), "Free surface effects on 2-D airfoils and 3-D wings moving over water", *Ocean Syst. Eng.*, **6**(3), 245-264.
- Bal, S., Atlar, M. and Usar, D. (2015), "Performance prediction of horizontal axis marine current turbines", *Ocean Syst. Eng.*, **5**(2), 125-138.

- Chang, J.F., Tsai, P.W., Chen, J.F. and Hsiao, C.T. (2014a), "The comparison between IABC with EGARCH in foreign exchange rate forecasting", *Proceedings of the 1st Euro-China Conference on Intelligent Data Analysis and Applications*, Shenzhen, China, June, 13-15.
- Chang, J.F., Yang, T.W. and Tsai, P.W. (2014), "Stock portfolio construction using evolved bat algorithm", *Proceedings of the 27th International Conference on Industrial, Engineering & Other Applications of Applied Intelligent Systems*, Kaohsiung, Taiwan, June, 3-6.
- Chen, C.W. (2014a), "Interconnected TS fuzzy technique for nonlinear time-delay structural systems", *Nonlinear Dynam.*, **76**(1), 13-22.
- Chen, C.W. (2014b), "A criterion of robustness intelligent nonlinear control for multiple time-delay systems based on fuzzy Lyapunov methods", *Nonlinear Dynam.*, **76**(1), 23-31.
- Chen, T., Khurram, S. and Cheng, C. (2019), "A relaxed structural mechanics and fuzzy control for fluid-structure dynamic analysis", *Eng. Comput.*, **36**(7), 2200-2219.
- Chen, T., Khurram, S. and Cheng, C. (2019), "Prediction and control of buildings with sensor actuators of fuzzy EB algorithm", *Earthq. Struct.*, **17**(3), 307-315. <https://doi.org/10.12989/eas.2019.17.3.307>.
- Chen, T. (2020), "LMI based criterion for reinforced concrete frame structures", *Adv. Concr. Constr.*, **9**(4), 407-412.
- Chen, T. (2020), "Evolved fuzzy NN control for discrete-time nonlinear systems", *J. Circuits Syst. Comput.*, **29**(1), 2050015.
- Chen, T. (2020), "On the algorithmic stability of optimal control with derivative operators", *Circuits Syst. Signal Process.*, doi:10.1007/s00034-020-01447-1.
- Chen, T. (2020), "An intelligent algorithm optimum for building design of fuzzy structures", *Iran J. Sci. Technol, Trans Civ. Eng.*, **44**, 523-531.
- Chu, S.C. and Tsai, P.W. (2007), "Computational intelligence based on behaviors of cats", *Int. J. Innovative Comput. Inform. Control*, **3**(1), 163-173.
- Chu, S.C., Tsai, P.W. and Pan, J.S. (2006), "Cat swarm optimization", *Proceedings of the Trends in Artificial Duman*, S. and Bal, S. (2017), "Prediction of the turning and zig-zag maneuvering performance of a surface combatant with URANS", *Ocean Syst. Eng.*, **7**(4), 435-460.
- Egresits, C., Monostori, L. and Hornyak, J. (1998), "Multistrategy learning approaches to generate and tune fuzzy control structures and their application in manufacturing", *J. Intel. Manufact.*, **9**, 323-329.
- Harms, V.W. (1979), "Design criteria for floating tire breakwaters", *J. Waterway Port Coast. Ocean Division*, **105**, 149-170.
- Kinaci, O.K., Kukner, A. and Bal, S. (2013), "On propeller performance of DTC post-panamax container ship", *Ocean Syst. Eng.*, **3**(2), 77-89.
- Lee, H.H. and Wang, W.S. (2001), "Analytical solution on the dragged surge vibration of tension leg platforms with wave large body and small body multi-interactions", *J. Sound Vib.*, **248**, 533-556.
- Lee, H.H. and Wang, W.S. (2003), "On the dragged surge vibration of twin TLP systems with multi-interactions of wave and structures", *J. Sound Vib.*, **263**, 743-774.
- Lewandowski, R., Bartkowiak, A. and Maciejewski, H. (2012), "Dynamic analysis of frames with viscoelastic dampers: a comparison of damper models", *Struct. Eng. Mech.*, **41**(1), 113-137.
- Liu, S.C. and Lin, S.F. (2013), "Robust sliding control for mismatched uncertain fuzzy time-delay systems using linear matrix inequality approach", *J. Chinese Inst. Engineers*, **36**(5), 589-597.
- Liu, X. and Zhang, Q. (2003), "New approach to H1 controller designs based on fuzzy observers for T-S fuzzy systems via LMI", *Automatica*, **39**, 1571-1582.
- Liu, Y.J. and Li, Y.X. (2010), "Adaptive fuzzy output-feedback control of uncertain SISO nonlinear systems", *Nonlinear Dynam.*, **61**, 749-761.
- Loria, A. and Nesic, D. (2003), "On uniform boundedness of parametrized discrete-time systems with decaying inputs: applications to cascades", *Syst. Control Lett.*, **94**, 163-174.
- Narendra, K.G., et al. (1998), "Intelligent current controller for an HVDC transmission link", *IEEE T. Power Syst.*, **13**, 1076-1083.
- Ott E., Grebogi, C. and Yorke, J.A. (1990), "Controlling chaos", *Phys. Rev. Lett.*, **64**, 1196-1199.
- Pardhan, P.M. and Panda, G. (2012), "Solving multiobjective problems using cat swarm optimization", *Expert*

- Syst. Appl.*, **39**, 2956-2964.
- Park, J., Kim, J. and Park, D. (2001), "LMI-based design of stabilizing fuzzy controllers for nonlinear systems described by Takagi–Sugeno fuzzy model", *Fuzzy Sets Syst.*, **122**, 73-82.
- Rabiei K, Ordokhani Y and Babolian E (2017) The Boubaker polynomials and their application to solve fractional optimal control problems. *Nonlinear Dynamics* 88(2): 1013-1026.
- Simoes, M.G., Bose, B.K. and Spiegel, R.J. (1997), "Design and performance evaluation of a fuzzy-logic-based variable-speed wind generation system", *IEEE T. Ind. Appl.*, **33**, 956-965.
- Sontag, E.D. (1989), "Remarks on stabilisation and input-to-state stability", *Proceedings of the 28th IEEE Conference on Decision Control*, Tampa, FL: 1376-1378.
- Steinberg A.M. and Kadushin, I. (1973), "Stabilization of nonlinear systems with dither control", *J. Math. Anal. Appl.*, **43**, 273-284.
- Sun, Q., Li, R. and Zhang, P. (2003), "Stable and optimal adaptive fuzzy control of complex systems using fuzzy dynamic model", *Fuzzy Sets Syst.*, **133**, 1-17.
- Takagi, T. and Sugeno, M. (1985), "Fuzzy identification of systems and its applications to modeling and control", *IEEE T. Syst. Man Cy.*, **15**, 116-132.
- Tsai, P.W., Kham, M.K., Pan, J.S. and Liao, B.Y. (2012), "Interactive artificial bee colony supported passive continuous authentication system", *IEEE Systems J.*, 1-11.
- Tsai, P.W., Pan, J.S., Liao, B.Y. and Chu, S.C. (2009), "Enhanced artificial bee colony optimization", *Int. J. Innov. Comput. Inform. Control*, **5**(12), 5081-5092.
- Tsai, P.W., Pan, J.S., Liao, B.Y., Tsai, M.J. and Vaci, I. (2012), "Bat algorithm inspired algorithm for solving numerical optimization problems", *Appl. Mech. Mater.*, **148-149**, 134-137.
- Tyan, C.Y., Wang, P.P. and Bahler, D.R. (1996), "An application on intelligent control using neural network and fuzzy logic", *Neurocomput.*, **12**, 345-363.
- Wang, H.O., Tanaka, K. and Griffin, M. (1996), "An approach to fuzzy control of nonlinear systems: stability and design issues", *IEEE T. Fuzzy Syst.*, **4**, 14-23.
- Xu, G., Hamouda, A.M.S. and Khoo, B.C. (2011), "Numerical simulation of fully nonlinear sloshing waves in three-dimensional tank under random excitation", *Ocean Syst. Eng.*, **1**(4), 355-372,
- Yang, C.K and Kim, M.H. (2011), "The structural safety assessment of a tie-down system on a tension leg platform during hurrrycane events", *Ocean Syst. Eng.*, **1**(4), 263-283.
- Zaky, M.A. (2018), "A Legendre collocation method for distributed{order fractional optimal control problems", *Nonlinear Dynam.*, **91**(4), 2667-2681.
- Zhu, Y., Zhang, Q., Wei, Z. and Zhang, L. (2013), "Robust stability analysis of Markov jump standard genetic regulatory networks with mixed time delays and uncertainties", *Neurocomput.*, **110**(13), 44-50.